Journal of Mining and Environment (JME) Vol. 18, No. 4, 2026, 1263-1283

Shahrood University of Technology

Journal of Mining and Environment (JME)

Journal homepage: www.jme.shahroodut.ac.ir

Iranian Society of Mining Engineering (IRSME)

Co-activation Mechanism of Lead Nitrate and Sodium Thioglycolate in Smithsonite Sulfidization Flotation

Ayman M. Ibrahim[1,2,3*], Han Wang[1], Dianwen Liu[1], Peilun Shen[1], Hassan A. Osman[3], Muhannad Alhaj[4], Mohamed A. Ibrahim[4], and Misbah Khalil[4]

1. State Key Laboratory of Complex Nonferrous Metal Resources Clean Utilization, Yunnan Key Laboratory of Green Separation and Enrichment of Strategic Metal Resources, Faculty of Land Resources Engineering, Kunming University of Science and Technology, Kunming 650093, Yunnan, PR China
2. Department of Mining Engineering, Faculty of Engineering Science, University of Nyala, Nyala 63311, PR Sudan
3. Department of Chemistry, Faculty of Education, University of Nyala, Nyala 63311, Sudan
4. Department of Mining Engineering, Faculty of Engineering Science, Omdurman Islamic University, Khartoum 14411, PR Sudan

Article Info

Received 27 October 2025
Received in Revised form 5 February 2026
Accepted 11 July 2026
Published online 11 July 2026

DOI: 10.22044/jme.2026.17042.3355

Keywords

Smithsonite
Co-activation mechanism
Lead nitrate
Sodium thioglycolate
Adsorption

Abstract

In this study, Pb^{2+} and STG were used as effective co-activation reagents before sodium sulfide treatment to assess their effect on smithsonite floatability. The flotation test results showed that sodium sulfide nonahydrate (SSN) and sodium diethyl dithiocarbamate (DDTC) concentrations significantly impacted floatability, achieving maximum recoveries of 89.32% and 93.19%, respectively. XPS analysis confirmed that Na_2S treatment introduced sulfur species onto the smithsonite surface, enhancing collector attachment and facilitating the formation of PbS and ZnS. FTIR analysis further substantiated that co-activation enhances DDTC adsorption via C=S vibrations, thereby increasing the number of active sites available for interaction with the collector relative to direct sulfidation. FESEM-EDS and AFM analysis at pH 9 confirmed that co-activation resulted in the formation of denser, cloud-like layers of PbS and ZnS on the surface. These layers improved flotation efficiency, increased hydrophobicity, and strengthened DDTC interaction, thus promoting flotation. Additionally, ToF-SIMS and EPMA analyses indicated higher Pb^{+} and S^{-} intensities in the co-activation system, confirming enhanced surface reactivity and substantiating the increased activity and diversity of sulfidation products. This study offers an effective approach to enhancing smithsonite flotation recovery by optimizing surface chemistry and collector attachment.

1. Introduction

Smithsonite is increasingly recognized as a valuable resource for zinc extraction, particularly as sulfide ore reserves diminish. Recent research has focused on developing innovative technologies for its recovery [1,2]. However, smithsonite can appear in various colors, including white, green, blue, yellow, and pink, influenced by trace elements such as copper, iron, or manganese [3,4]. Recently, it has attracted attention for its environmental potential, including its role in zinc recycling and as a material for carbon capture, thanks to its ability to absorb carbon dioxide. In the past, zinc sulfide ores exhibited superior floatability compared to oxide ores during industrial production. However, these resources are steadily depleted as zinc sulfide ores have been extensively mined and utilized [5–9]. Consequently, the effective utilization of zinc oxide minerals has become a crucial strategy for supplementing zinc metal supply [10–12]. If the zinc oxide ore contains minimal carbonate gangue minerals, the zinc can be leached directly with acid [13,14]. However, the colloidal siliceous material produced by silicate minerals complicates filtration and hinders subsequent zinc extraction. Ammonia selectively leaches zinc oxide but is ineffective for dissolving zinc in silicates, resulting in low leaching rates [15]. These challenges hinder the

Corresponding author: aymanzrouge@gmail.com (A.M. Ibrahim)

industrial hydrometallurgical processing of zinc oxide ore.

Currently, due to its relatively low zinc content compared to higher-grade ores, low-grade smithsonite is typically recovered using various flotation methods, including fatty acid flotation, flocculation flotation,

sulfidization amine flotation, chelating flotation, cationic/anionic collector flotation, and sulfidation xanthate flotation. Fatty acid flotation, which uses anionic collectors such as fatty acids, is particularly effective for ores containing siliceous and argillaceous gangue [16–19]. The study conducted by Liao et al. [20] examined the effectiveness of a mixed collector system consisting of dodecyl amine (DDA) and sodium diethyl dithiocarbamate (DDTC) in enhancing smithsonite flotation. The mixture improved flotation efficiency, showing synergistic effects, increased hydrophobicity, and multilayer adsorption on the smithsonite surface, as verified through various methods. Sulfidization flotation is a widely used technique for extracting base metals from oxide ores, particularly zinc, copper, and lead [21]. In this process, sodium sulfide nonahydrate (SSN) is commonly used as the sulfidizing agent. For smithsonite, sulfidization involves introducing sulfur or sulfur-containing compounds, such as hydrogen sulfide (H_2S) or sulfur dioxide (SO_2), to convert zinc oxide into zinc sulfide (ZnS), thereby enhancing surface characteristics and floatability during flotation [22–25]. Zinc sulfide is more hydrophobic, which enhances its separation from gangue minerals during flotation and significantly reduces collector consumption [26]. Wu et al. [27] investigated the effect of sulfur ion adsorption on smithsonite during sulfidization in the extraction of oxidized zinc. Their findings revealed sulfur adsorption, alterations in surface charge, and the development of a ZnS film, with sulfur ions integrating into the mineral's crystal structure. Although smithsonite is a semi-soluble mineral that releases Zn^{2+} in solution, it interacts with OH^- in alkaline conditions, as given in Equations (1) – (6) bellow:

$$Zn^{2+} + 2OH^- \leftrightharpoons Zn(OH)_{2(s)} \quad (1)$$

The reaction product, $Zn(OH)_2(s)$, forms a hydroxylated surface on the smithsonite in the pulp solution [28]. In the alkaline solution, the sulfidization process is considered an ion-exchange between HS^-, S^{2-}, CO_3^{2-}, and OH^- on the smithsonite surface [27,29,30].

$$Na_2S \Leftrightarrow 2Na^+ + S^{2-} \quad (2)$$

$$S^{2-} + H_2O \Leftrightarrow HS^- + OH^- \quad (3)$$

$$ZnCO_{3(s)} + HS^- \leftrightharpoons ZnS_{(s)} + HCO^- \quad (4)$$

$$ZnCO_{3(s)} + S^- \leftrightharpoons ZnS_{(s)} + {CO_3}^{2-} \quad (5)$$

$$Zn(OH)_{2(s)} + HS^- = ZnS_{(s)} + H_2O + OH^- \quad (6)$$

Zhang et al. [31,32] studied the effect of Pb ion pre-modification on smithsonite during sulfidization-xanthate flotation. They found that Pb pre-modification improved floatability by forming Pb carbonates on the mineral surface, which reacted with sulfur to form Pb–S species. This enhanced the stability of the sulfide layer and improved flotation recovery, without significantly increasing sulfur ion adsorption. Luo et al. [33] used density functional theory calculations to investigate the depression effect of Ca ions on the sulfidization of smithsonite. Their results showed that Ca ion adsorption significantly reduced the reactivity of the smithsonite surface. The presence of Ca ions weakened Ca-S bonds and made the hydration shell harder to break, inhibiting the adsorption of HS, thus explaining the Ca ions' negative effect on smithsonite sulfidization. Jia et al. [34] found that smithsonite's natural hydrophilicity makes flotation recovery challenging. Conditioning with sodium sulfide alone was ineffective, but combining S(II), Pb(II), and xanthate improved flotation, achieving a 95.8% recovery. Analytical techniques revealed that S(II) treatment formed an amorphous ZnS layer, while S(II) and Pb(II) created a cubic PbS layer, aiding flotation. Another study by Bai et al. [35] investigated the promotion of smithsonite sulfidization by adding ammonium chloride (NH_4Cl). Their findings show that NH_4Cl enhances flotation recovery by ~17%, increases the surface concentration of zinc sulfide species, and improves sulfidization via ion-exchange and adsorption of sulfide and xanthate species, as confirmed by various experimental analyses. Feng et al. [36] used lead ions to activate the surface flotation of smithsonite and reported that the Pb^{2+} pre-treatment enhanced surface sulfidization, increased xanthate adsorption, and enhanced hydrophobicity more than direct sulfidization.

Furthermore, a few studies have explored the use of STG as an enhancer reagent. For example, Xiao et al. [37] investigated the enhancement of galena separation from sphalerite using CaO and sodium thioglycolate as synergistic enhancers and found that the process achieved high galena recovery and low sphalerite recovery. Mechanistic

studies showed that CaO and sodium thioglycolate effectively depressed sphalerite flotation. Although Pb^{2+} has been extensively studied as an activator in flotation processes, the combination of Pb^{2+} and STG as a co-activation mechanism in sulfidized smithsonite flotation has not been fully explored. Previous studies have focused on individual activators such as Pb^{2+} without examining the synergistic effects of combining Pb^{2+} with STG. This study, however, introduces a novel co-activation system in which Pb^{2+} and STG work together to enhance the flotation of smithsonite more effectively than either Pb^{2+} or STG alone. The combined mechanism, particularly its impact on sulfide interactions and surface activation, has not been investigated previously. Thus, this study offers new insights into flotation chemistry and advances methods for improving mineral separation.

This study investigates the functionalization of the co-activation mechanism on sulfidized smithsonite using lead nitrate ($Pb(NO_3)_2$) and sodium thioglycolate (STG) to enhance adsorption performance through various analyses, with DDTC as the collector. Additionally, the changes in the surface structure, sulfidization behavior, and sulfide layer stability of smithsonite before and after adsorption were analyzed using various techniques, including flotation experiments, X-ray photoelectron spectroscopy (XPS), Time-of-Flight secondary ion mass spectrometry (ToF-SIMS), electron probe micro-analyzer (EPMA), atomic force microscopy (AFM), field emission scanning electron microscopy-energy dispersive spectroscopy (FESEM-EDS), Fourier transform infrared spectroscopy (FT-IR), and adsorption experiments. These results will pave the way for understanding the co-activation mechanism of adsorption systems and their relation to the sulfidization behavior in smithsonite flotation.

2. Materials and methods

2.1. Materials and reagents

The smithsonite ore sample was sourced from Yunnan Province, China. The mineral sample was first crushed to the desired particle size and then sieved into a specific, homogenized size fraction, typically 38-74 μm, to optimize flotation conditions. Analytical-grade Lead Nitrate ($Pb(NO_3)_2$) and Sodium Thioglycolate (STG) were used as co-activation reagents, each at a concentration of 3×10^{-4} mol/L, while sodium sulfide nonahydrate (SSN, $Na_2S{\cdot}9H_2O$ = 2×10^{-3} mol/L) was employed in the sulfidation steps, and sodium diethyldithiocarbamate (1×10^{-4} mol/L DDTC) served as the collector. All reagents were freshly prepared to maintain their stability. The pH was adjusted using diluted hydrochloric acid (HCl) to lower the pH or diluted sodium hydroxide (NaOH) to raise it, depending on the flotation requirements. Deionized water (DI) with a resistivity of 18.25 MΩ·cm was used in all tests. The X-ray fluorescence (XRF) results for pure smithsonite are shown in Table 1.

Table 1. XRF analysis results of pure smithsonite ore.

Element	O	Ca	Mn	Fe	Zn	Cd	Pb
Conc. (%)	41.43	0.98	0.16	0.51	53.03	0.56	0.28

2.2. Flotation studies

Flotation experiments were conducted using the XFGC-II flotation machine from Jilin Exploration Machinery Plant, Changchun, China. 2 grams of the smithsonite sample and 36 mL of deionized water were added to the flotation cell and stirred for 2 minutes. $Pb(NO_3)_2$ and STG solutions were then added to the pulp, and the mixture was conditioned for 5 minutes each. As needed, the pH was adjusted using pH modifiers (dilute NaOH or HCl solutions). The pulp was treated sequentially with Na_2S and DDTC (collector) for 5 and 2 minutes, respectively. Methyl Isobutyl Carbinol (MIBC, approximately 50 mg/L) was added to the pulp and allowed to react for 1 minute. After 3 minutes of aeration, the floated product was collected. Both the floated product and residue were dried and weighed to determine their respective masses. The recovery of smithsonite (R) was calculated using Equation (7) as follows:

$$R = \frac{Q_1(floated\ product)}{Q_1(floated\ product)+Q_2(residue)} \times 100\% \qquad (7)$$

Where are:

R– represents recovery,

Q_1 and Q_2 – denote the masses of the float and residue products.

Each experiment was performed in triplicate, and the average flotation recovery was calculated. The entire process (as shown in Figure 1).

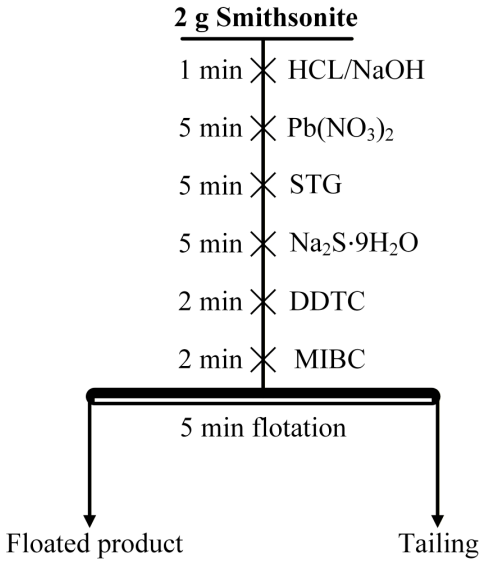

Figure 1. Flowsheet of flotation experiments.

2.3. FESEM-EDS analysis

FESEM (Nova Nano SEM 450, USA) and EDS (Oxford X−Max) were used to examine the surface morphology and elemental composition of the sulfidized smithsonite before and after co-activation. The elements analyzed included Cu, O, C, and S through EDS surface analysis. For sample preparation, the samples were carefully ground into a fine powder and sieved to a suitable particle size. A 2-gram representative sample was placed into a laboratory glass beaker containing 36 ml of deionized water at pH 9. The reagents were added as needed, and the sample was conditioned for 5 minutes before being dried in a vacuum oven. The treated samples were then placed under vacuum and coated with platinum before conducting the FESEM-EDS analysis.

2.4. AFM analysis

Atomic force microscopy (AFM) was used to characterize changes in the surface properties of sulfidized smithsonite before and after the adsorption of $Pb(NO_3)_2$ and STG solutions as co-activation reagents. For test preparation, a large smithsonite block sample was cut into small pieces and polished to obtain a flat surface. The sample was then immersed in the reagents for 10 minutes under each condition and allowed to dry naturally. AFM imaging was performed using a Bruker Dimension Icon AFM (Germany) to identify adsorption sites and analyze surface heterogeneity, both of which are essential for understanding how co-activation reagents influence the flotation process.

2.5. XPS analysis

XPS analysis was performed using a PHI5000 Versa Probe II instrument (ULVAC−PHI Inc., Chigasaki, Kanagawa, Japan). The sample treatment conditions were identical to those used in the flotation tests. XPS was then employed to investigate changes in the chemical state of the smithsonite surface after treatment with various reagents. The system is equipped with a monochromatic Al Kα X-ray source (1486.6 eV) for full- and narrow-spectrum scanning. The C1s peak (284.80 eV) was used to calibrate the binding energy. Data were compiled and processed from the peak region using MultiPak software.

2.6. ToF-SIMS analysis

ToF-SIMS analysis (Ion-ToF IV, Munster, Germany) was employed to characterize the smithsonite sample surfaces under various conditions. The primary ion beam (25 keV Bi_3^+) operated in static mode with a pulsed beam current of 1.12 pA. Each sample was analyzed over a 150 µm × 150 µm area for spectral acquisition. A 1 keV O_2 sputter ion with a current of 227.79 nA was used, and the sputter area was 500 µm × 500 µm. Before statistical analysis (mean analysis), the intensities of key secondary ions in the ToF-SIMS spectra were normalized to the total ion yield. The analysis was conducted in a vacuum at a pressure of 10^{-7} Pa or lower, with sample charges neutralized by an electron flood gun.

2.7. EPMA analysis

The composition of smithsonite was analyzed using an EPMA-1720 (Shimadzu Co. Ltd., Japan), with an accelerating voltage of 15 kV and a probe current of 20 nA. The study focused on examining surface variations of smithsonite, particularly the effects of surface enhancement through activation reagents. For preparation, 0.5 g of pure smithsonite powder was placed in a laboratory beaker with co-activation reagents and treated for 10 minutes each, prior to sulfidization. The samples were then dried in a vacuum at 25°C. Prior to EPMA measurement, each sample was coated with carbon. Elements such as sulfur, carbon, lead, zinc, and oxygen were analyzed on the surface.

2.8. ICP analysis

The Inductively Coupled Plasma instrument (7700x, Agilent Technologies, USA) was used to determine sulfur concentrations in smithsonite samples following sulfidization and co-activation

with Pb^{2+} and STG. Briefly, approximately 2 g of smithsonite was added to 36 mL of deionized water in a 50 mL conical beaker. The mixture was stirred at 1200 rpm using a magnetic stirrer and conditioned with the required reagents for specific durations (2, 4, 5, 6, 8, and 10 minutes). After treatment, 2 mL of the supernatant was collected, centrifuged to remove particulates, and diluted for sulfur concentration measurement via ICP-OES. Samples were then centrifuged at 4,000 rpm for 30 minutes. Each experiment was performed in triplicate, and the average value and standard deviation were reported.

2.9. FT-IR analysis

An infrared spectrometer (Nicolet iS50, Thermo Fisher Scientific, USA) was used to identify and characterize the interactions between the reagents (lead nitrate and sodium thioglycolate) and the sulfidized smithsonite surface. Smithsonite samples were ground to a −5 μm size fraction. A 2-gram sample of smithsonite was mixed with deionized water in a volumetric flask and stirred. NaOH and HCl solutions were added to adjust the pH to around 9. The required reagents were added to the flotation suspension, each for 10 minutes. Afterwards, the suspension was filtered and dried at 45°C in a vacuum oven before FT-IR analysis. FT-IR spectra were recorded from 400 to 4000 cm^{-1}.

3. Results and discussion

3.1. Flotation test results

Figure 2 illustrates the significant influence of sodium sulfide (Na_2S) and DDTC concentrations on smithsonite floatability. At a fixed DDTC concentration of 2.5×10^{-3} mol/L, the recovery of smithsonite varied as a function of sodium sulfide nonahydrate (SSN) concentration (as shown Figure 2a). Recovery was low at low Na_2S concentrations and in the absence of Pb^{2+} and STG, which can be attributed to insufficient sodium sulfide concentration to improve smithsonite floatability. The recovery peaked at 52.34% with 2×10^{-3} mol/L Na_2S, indicating that an optimal Na_2S concentration effectively sulfidizes the smithsonite surface, thereby enhancing collector attachment and improving floatability. However, as Na_2S concentration increased further, recovery steadily declined, reaching 19.66% at 3.5×10^{-3} mol/L, suggesting that excessive Na_2S impairs flotation performance, likely by promoting the formation of surface species that hinder collector attachment.

Upon adding Pb^{2+} and STG before sulfidization, flotation recovery was significantly higher than that achieved through direct sulfidization, reaching a maximum of 89.32% at the same Na_2S concentration. This enhancement is attributed to the improved activation of the smithsonite surface, which facilitates better collector attachment and promotes more effective flotation. However, when Na_2S concentration exceeded the optimal point, recovery sharply decreased to 35.47%, indicating that excessive sodium sulfide interferes with flotation by disrupting surface interactions or promoting the formation of undesirable compounds.

Figure 2b illustrates the effect of DDTC concentration on smithsonite floatability, showing a positive correlation between DDTC concentration and recovery. In the presence of Na_2S, within the DDTC concentration range of 1×10^{-4} to 2.5×10^{-3} mol/L, the highest recovery reached 65.08%. Beyond this point, further increases in DDTC concentration did not significantly improve floatability, suggesting saturation. When smithsonite was co-activated with Pb^{2+} and STG prior to Na_2S treatment within the same DDTC concentration range, the maximum recovery achieved was 93.19%, which was higher than that obtained through direct sulfidization. This improvement indicates that the co-activation system enhances flotation by promoting the formation of more Pb-S species on the mineral surface, which supports the co-activation mechanism of lead nitrate and sodium thioglycolate. This concentration range is considered optimal, indicating high collector efficiency. However, as DDTC concentration increased, recovery initially increased and then stabilized, likely due to saturation of the mineral surface's active sites.

3.2. XPS test results

Figure 3 shows the high-resolution XPS spectra and elemental atomic concentrations on the smithsonite surfaces under different conditions. The energy spectrum of the pure smithsonite surface reveals characteristic peaks for O, C, and Zn, with atomic concentrations of 56.07% for O 1s, 17.96% for C 1s, and 25.97% for Zn 2p. The addition of Na_2S introduced a measurable concentration of S 2p on the surface, while the concentrations of O 1s, C 1s, and Zn 2p decreased to 49.98%, 17.91%, and 25.96%, respectively. A new atomic concentration of S 2p, approximately 6.15%, was detected on the surface, likely from

Na_2S. This increase in sulfur content enhances the collector's adsorption reactivity on the smithsonite surface.

Following co-activation of smithsonite with Pb^{2+} + STG and sulfidization, the intensity of the S 2p peaks further increased, reaching an atomic concentration of about 7.69% compared to the Na_2S treatment, indicating the presence of more sulfide species. Additionally, a new Pb 4d peak was detected at approximately 6.28% atomic concentration. Thus, the Pb^{2+} + STG co-activation system promotes sulfidization on the smithsonite surface, creating favorable conditions for enhanced collector interactions.

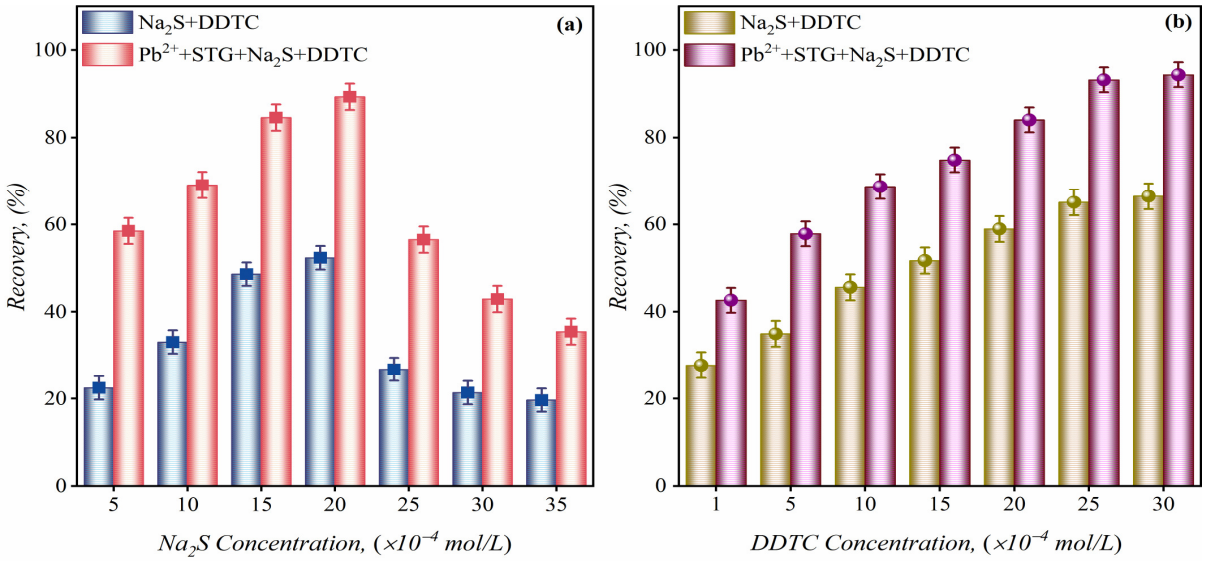

Figure 2. Flotation recovery of sulfidized smithsonite as a function of (a) Na_2S concentration and (b) DDTC concentration.

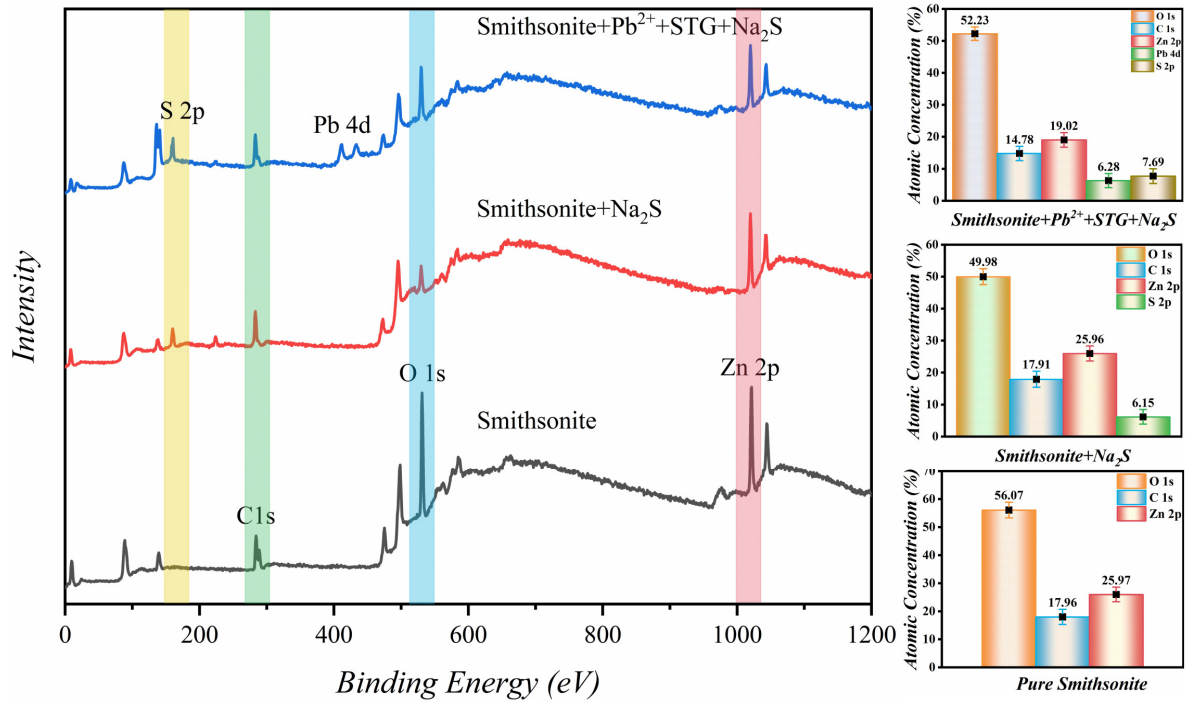

Figure 3. XPS survey spectra and atomic concentrations on the smithsonite surfaces.

Figure 4 shows the Zn 2p spectra of pure smithsonite surfaces subjected to different treatments. For the smithsonite surface treated with DI water (as shown in Figure 4a), a pair of symmetric Zn 2p characteristic peaks (Zn $2p_{1/2}$ and Zn $2p_{3/2}$), which exhibit identical chemical

properties, is observed. The binding energies for Zn $2p_{1/2}$ and Zn $2p_{3/2}$ are 1045.27 eV and 1022.12 eV, respectively. After treating the smithsonite with Na_2S (as shown Figure 4b), the Zn $2p_{3/2}$ peak shifts by −0.17 eV, suggesting a subtle interaction between the sulfide treatment and the zinc on the surface, indicating a slight effect on the electronic environment of the zinc ions. However, when a co-activation process involving Pb^{2+} and STG is applied prior to sulfidization (as shown in Figure 4c), a more significant shift is observed. Specifically, the Zn $2p_{3/2}$ peak shifts from 1021.95 eV to 1021.74 eV, a change of −0.21 eV. This leftward shift indicates a stronger interaction or alteration in the electronic structure of the zinc, likely due to the Pb^{2+}/STG co-activation.

Two pairs of characteristic S 2p peaks (S $2p_{3/2}$ and S $2p_{1/2}$) are fitted to the S 2p spectra of the smithsonite surface before and after treatment under different conditions. For smithsonite treated with DI water (as shown in Figure 4d), no S 2p peak is detected, indicating that no sulfur-containing species were formed on the surface during the treatment. After Na_2S sulfidization (as shown in Figure 4e), the S 2p peak was fitted with two distinct doublets. The first doublet, with binding energies of 161.19 and 162.38 eV for the S $2p_{3/2}$ and S $2p_{1/2}$ levels, respectively, separated by 1.18 eV and exhibiting an intensity ratio of 2:1, corresponds to sulfur in monosulfide form [38]. This indicates the formation of Zn–S surface components, suggesting that the sulfidization process successfully facilitated interaction between sulfur and zinc. The second doublet peaks were observed at 162.27 eV and 163.68 eV, which were attributed to the formation of polysulfides [39,40]. When smithsonite was co-activated with the Pb^{2+}+STG system (as shown in Figure 4f), the S distribution ratio in polysulfides increased, suggesting that the co-activation mechanism enhanced the formation of polysulfides on the sulfurized smithsonite surface and accelerated sulfidization reaction. Additionally, the binding energy shifted slightly to lower values (from 162.27 eV to 162.23 eV and from 161.19 eV to 161.03 eV), corresponding to the S $2p_{3/2}$ peaks of the Zn–S and Pb–S components, further indicating the involvement of both zinc and lead in the sulfidization process [39,41]. This may be another factor boosting the floatability of smithsonite after the co-activation–sulfidization process by enhancing its hydrophobicity and increasing its surface reactivity with the collector.

Figure 5 and Table 2 show the XPS spectra of O 1s on the smithsonite surface before and after treatment with various reagents. The peaks at 531.62 eV and 532.87 eV correspond to CO_3^{2-} and –OH groups, respectively [42–44]. For smithsonite treated with DI water, the relative amounts of CO_3^{2-} and –OH were 86.19% and 13.81% (as shown in Figure 5a). After Na_2S treatment, these values shifted to 88.95% and 11.05% (as shown in Figure 5b). This indicates that SSN treatment increases the proportion of CO_3^{2-} while slightly reducing the number of –OH groups, suggesting modifications in surface chemistry and a potential change in the mineral's reactivity. When co-activated with Pb^{2+} + STG prior to sulfidization (as shown in Figure 5c), the percentages of CO_3^{2-} and –OH were 87.56% and 12.44%. Compared to Na_2S treatment, the changes in CO_3^{2-} and –OH contents were minimal, indicating that co-activation with Pb^{2+} + STG + Na_2S had little impact on the O species on the smithsonite.

The Pb 4d spectra, both before and after co-activation with Pb^{2+}, STG, and sulfidization, were analyzed to study the effect of the co-activation system on the smithsonite surfaces. The spectrum of the pure smithsonite surface (as shown in Figure 5d) shows no distinct Pb 4d peak, confirming the sample's high purity. After adding SSN (as shown in Figure 5e), no significant Pb 4d peak was detected, indicating that sodium sulfide does not contain Pb in its chemical structure. Following treatment with the Pb^{2+} + STG + Na_2S system, two pairs of peaks appeared in the smithsonite spectrum, attributed to the –Pb–S and –Pb–O components [45,46].

The peak at 411.19 eV corresponds to Pb in the –Pb–S species, while the peak at 413.79 eV is attributed to Pb in the Pb–O species (as shown in Figure 5f). The proportions of –Pb–S and –Pb–O in the total Pb component were 41% and 59%, respectively. These ratios reflect the dominance of each bonding type, suggesting the formation of new Pb-containing surface components. Compared with SSN treatment alone, these findings confirm the formation of PbS, thereby increasing the number of active surface sites available for interaction with the collector.

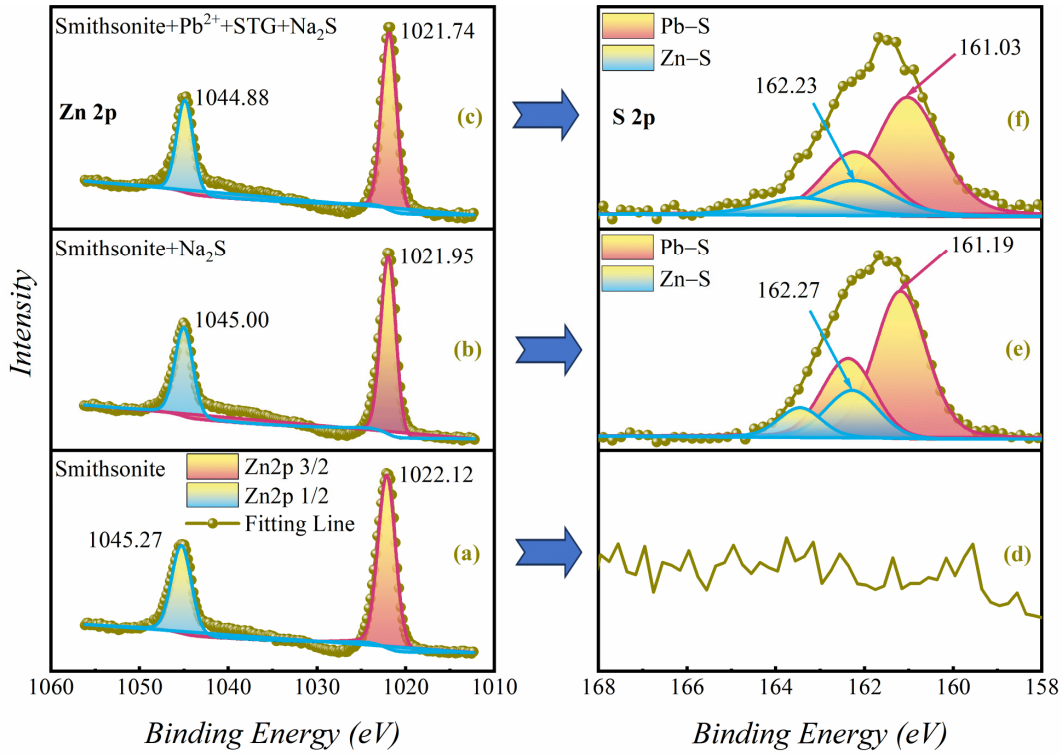

Figure 4. Zn 2p and S 2p XPS spectra of pure smithsonite treated with (a) Water, (b) Na_2S, and (c) Pb^{2+}+ STG +Na_2S

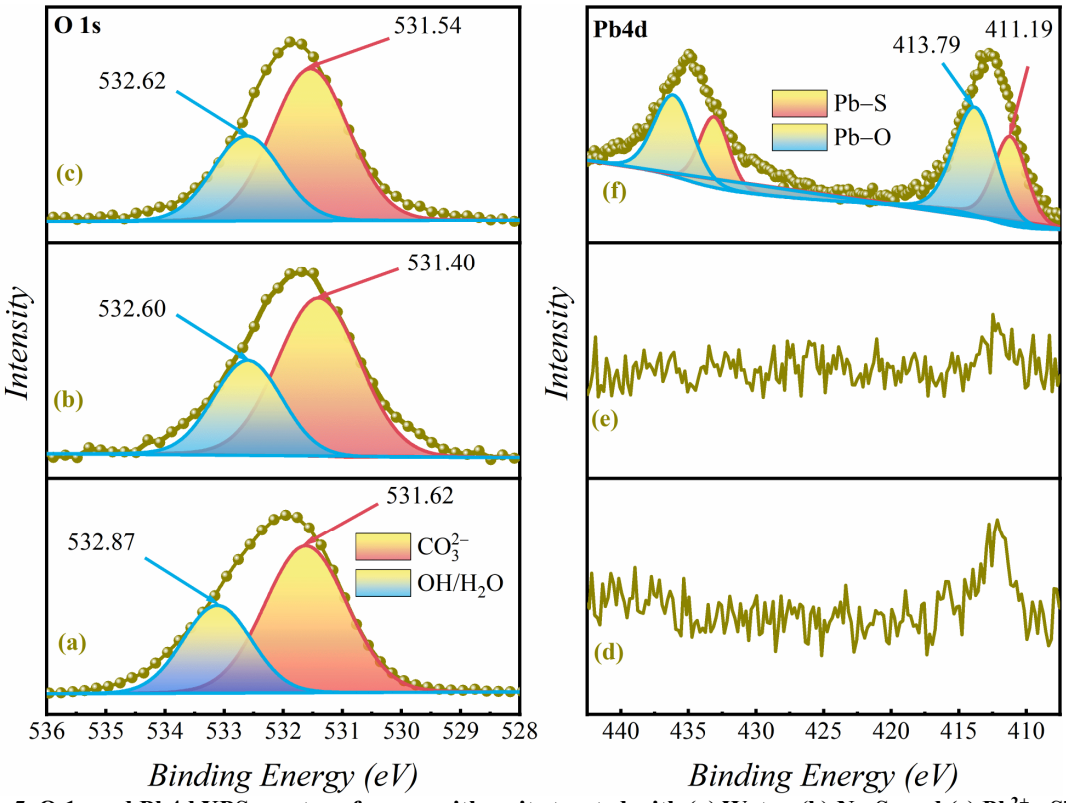

Figure 5. O 1s and Pb4d XPS spectra of pure smithsonite treated with (a) Water, (b) Na_2S, and (c) Pb^{2+}+ STG + Na_2S.

Table 2. O1s species contents of (a) Water, (b) Na_2S, and (c) Pb^{2+}+ STG + Na_2S.

Sample	Species	Species distribution (%)
(a)	CO_3^{2-}	86.19
	$-OH$	13.81
(b)	CO_3^{2-}	88.95
	$-OH$	11.05
(c)	CO_3^{2-}	87.56
	$-OH$	12.44

3.3. FESEM-EDS test results

FESEM characterization was conducted to investigate the sulfidization process behavior of Na_2S on smithsonite samples before and after co-activating the surface with the Pb^{2+} and STG system, as shown in (as shown in Figure 6). For the pure smithsonite sample treated with DI water at 50,000X magnification, the FESEM images revealed a smooth and clean surface that can be clearly observed in the mapping [45], as shown in Figure 6a, indicating the surface purity of the smithsonite sample, along with elemental surface morphology maps of Zn, O, C, and Ca. No sulfur was detected under these conditions. Following the addition of Na_2S in the smithsonite flotation test (as shown in Figure 6b), the overall shape of the smithsonite surface changed relatively little, with small aggregate films observed that may contain Zn-S species formed on the surface. In this test, under the same magnification, the color of the elemental morphology maps (Zn, O, C) also showed slight changes to darker colors, with a newly detected S element map on the surface, suggesting that the sulfidization process occurred, leading to the formation of sulfur-containing species on the surface compared to the DI water treatment [21].

After co-activating smithsonite with the Pb^{2+} and STG system prior to sulfidization (as shown in Figure 6c), the FESEM image at 50,000X magnification showed that the surface was fully covered with aggregate films, forming dense, cloud-like layers. These layers likely contain Zn-S and Pb-S species, indicating that the co-activation process promotes the formation of sulfur-rich compounds, enhancing surface reactivity and modification. Elemental mapping of Zn, O, Pb, and S confirmed that the surface was nearly entirely covered by these cloud-like layers, correlating with increased sulfur content and improved hydrophobicity. Compared to the Na_2S system, the Pb^{2+}+STG flotation system forms denser, cloud-like layers of PbS and ZnS on the smithsonite surface, further enhancing interaction between the mineral and the DDTC collector, thereby promoting smithsonite flotation. These findings are consistent with the ToF-SIMS analysis results.

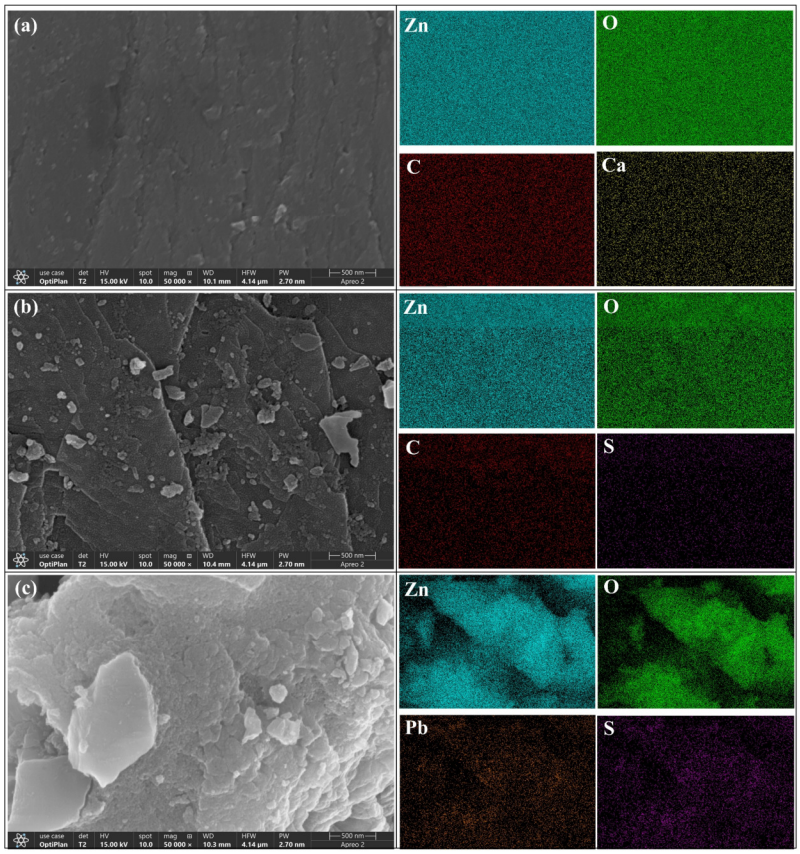

Figure 6. Surface morphologies of pure smithsonite treated with (a) Water, (b) Na_2S, and (c) Pb^{2+}+ STG + Na_2S.

To further investigate the sulfidization process and co-activated sulfidization with Pb^{2+} and STG on the smithsonite samples, EDS scanning analysis was performed (as shown in Figure 7). For smithsonite treated with only DI water (as shown in Figure 7a), the elemental contents of Zn, O, C, and Ca were 50.4%, 36.1%, 12.8%, and 0.7%, respectively, confirming that no reagents were added under these conditions.

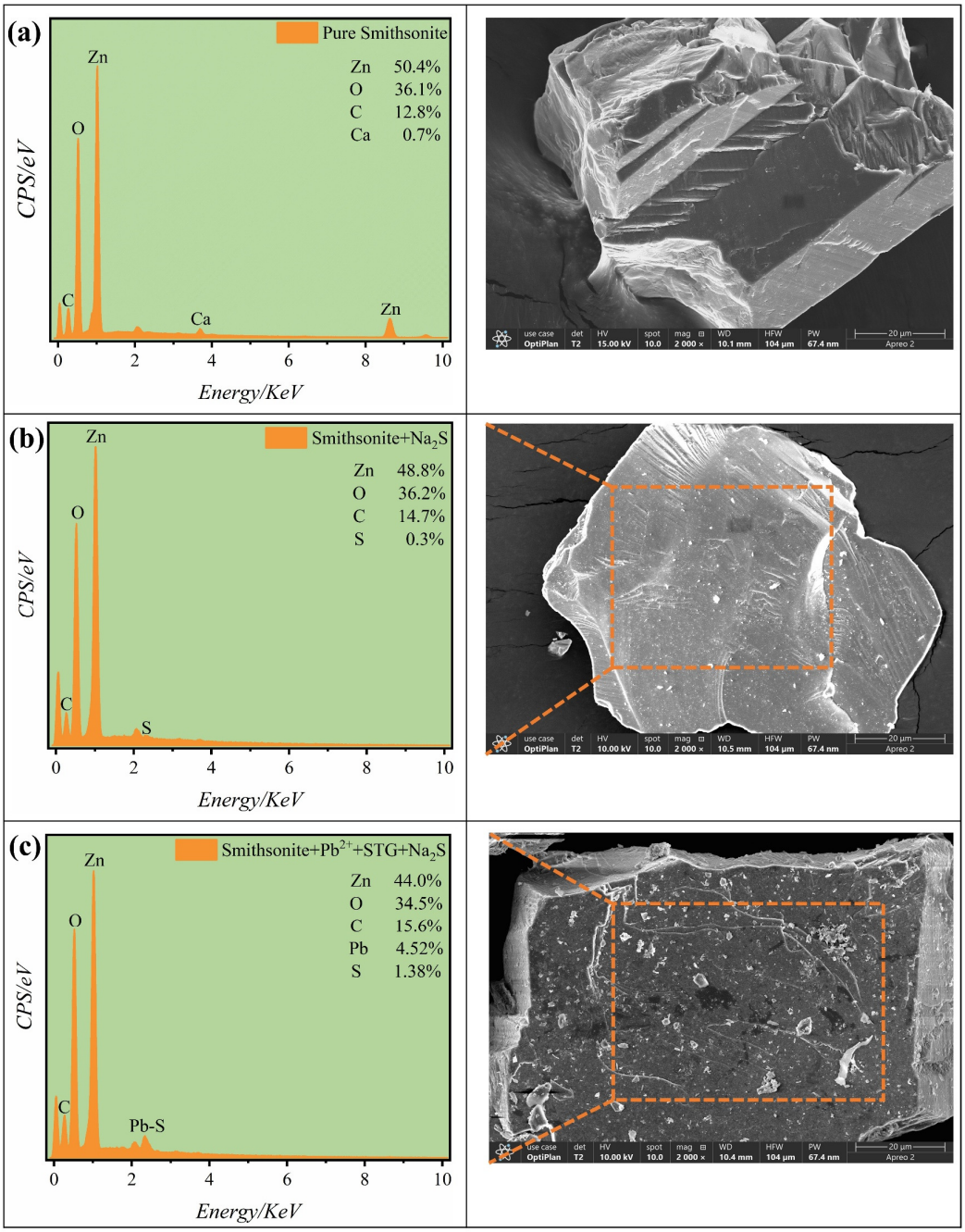

Figure 7. EDS spectra of pure smithsonite treated with (a) Water, (b) Na_2S, and (c) Pb^{2+}+ STG + Na_2S.

After Na_2S treatment, semi-quantitative analysis revealed a new sulfur (S) peak at 0.3%, indicating that sulfidization occurred on the smithsonite surface, likely forming sulfur-containing compounds such as Zn-S [47]. The peaks for Zn, O, and C were detected at 48.8%, 36.2%, and 14.7%, respectively (as shown in Figure 7b). Compared to the DI water treatment, the Zn content decreased by 1.6%, while the C content increased by 1.9%. These changes reflect

the chemical interactions between the surface and Na_2S, influencing the elemental composition of the treated surface.

In contrast, after co-activation of smithsonite with Pb^{2+} and STG prior to sulfidization (as shown in Figure 7c), the elemental contents of S, O, and C increased to 1.38%, 34.5%, and 15.6%, respectively. Additionally, a new Pb peak was detected in the EDS analysis at 4.52%. These results demonstrate that effective sulfidization occurred after co-activation, leading to the formation of more active sites, such as Pb-S and Zn-S compounds, compared to direct sulfidization. The apparent zinc content on the surface decreased by 4.8% compared to direct sulfidization and by 6.4% compared to DI water treatment, indicating that the decrease in Zn percentage is due to the formation of Zn-S and Pb-S compounds, which reduce zinc availability on the surface.

3.4. AFM test results

At pH 9, high-resolution two-dimensional (2D) and three-dimensional (3D) topographic images of (a) pure smithsonite, (b) sulfidized smithsonite, and (c) smithsonite treated with Pb^{2+} and STG before Na_2S treatment were captured using atomic force microscopy (AFM). As shown in Figure 8 and Table 3, AFM analysis typically uses the maximum height roughness (Rmax), average surface roughness (Ra), and root-mean-square roughness (Rq) to characterize surface roughness [48,49]. The initial smithsonite surface appeared flat and smooth, with grooves visible across the surface (as shown in Figure 8a). This smoothness suggests the sample is ideal for demonstrating smithsonite's surface sulfidization strength. The low maximum roughness (Rmax = 22 nm), along with the average surface roughness (Ra = 14.2 nm) and root-mean-square roughness (Rq = 17.1 nm), indicates a relatively even surface with minimal elevation variations, despite the presence of grooves. For the smithsonite surfaces treated with SSN (as shown in Figure 8b), the surface roughness parameters, including Rmax = 267 nm, Ra = 28.1 nm, and Rq = 35 nm, increased notably compared to those of pure smithsonite, suggesting that sulfidization occurred but was incomplete under these conditions [50].

After treatment with Pb^{2+}, STG, and Na_2S (as shown in Figure 8c), the surface roughness further increased, with Rmax = 346 nm, Ra = 32.5 nm, and Rq = 41.5 nm, all higher than those observed in direct sulfidization. This change indicates a significant alteration in surface texture, suggesting that the treatment had a noticeable impact on the surface morphology, resulting in more pronounced surface features. At this stage, the smithsonite surface has reached its maximum sulfidization saturation, making further sulfidization more difficult [51], which indicates that the treatment has optimized the sulfidization process. Unlike conventional sulfidization flotation, smithsonite treated with co-activation shows a substantial increase in surface Rmax ($\triangle$Rmax = +79 nm), suggesting that a more stable surface layer may contain compounds such as lead sulfide (PbS) and zinc sulfide (ZnS). This suggests that co-activation results in a more consistent and uniform surface modification than traditional sulfidization methods, facilitating the subsequent reaction of smithsonite with the collectors.

Table 3. Surface roughness of smithsonite treatment under various conditions.

Roughness	Water treatment	Na_2S treatment	Pb^{2+}+ STG + Na_2S treatment
Rmax (nm)	22	267	346
Ra (nm)	14.2	28.1	32.5
Rq (nm)	17.1	35	41.8

3.5. ToF-SIMS test results

The ToF-SIMS analysis was employed to characterize the adsorption characteristics of various reagents on smithsonite surfaces (as shown in Figure 9). For smithsonite treated with DI water at pH 9 (as shown in Figure 9a), the signal intensities of Zn^+, Pb^+, S^-, and CO_3^- ions were 4.219e+005, 1.411e+004, 1.085e+005, and 3.200e+005, respectively. This result suggests that the low signal intensities reflect an absence of reagent interaction or adsorption on the smithsonite surface. In contrast, after Na_2S sulfidization of smithsonite, the signal intensities of Pb^+, S^-, and CO_3^- ions slightly increased, with values of 2.571e+004, 2.981e+005, and 5.022e+005, respectively, compared to previous analyses. This result suggests that the smithsonite surface absorbed only a limited amount of Na_2S (as shown in Figure 9b), where a noticeable increase in sulfur intensity is observed following the SSN treatment at pH 9. Additionally, the intensity of Zn^+ ions decreased to 3.342e+005 compared to pure

smithsonite, indicating that some of the zinc on the surface may have been displaced or altered during the treatment process.

Following co-activation with Pb^{2+} and STG before sulfidization (as shown in Figure 9c), this condition indicates that these reagents effectively react with the active sites on the smithsonite surface, thereby enhancing its reactivity. Moreover, the signal intensities of Pb^{+} and S^{-} significantly increased to 7.590e+004 and 6.821e+005, respectively. In contrast, the intensities of CO_3^{-} and Zn^{+} gradually decreased to 2.940e+005 and 2.519e+005 compared to the smithsonite treated only with Na_2S. This change indirectly confirms the significant adsorption of Pb^{2+} and STG on smithsonite surfaces, supporting their absorption in the co-activation system. The results indicate that the activity and quantity of sulfidized components on the mineral surface increased, in accordance with the XPS results [52,53], thereby enhancing the interaction between the DDTC collector and the smithsonite surface.

Figure 10 shows the normalized peak intensities of Zn^{+}, Pb^{+}, S^{-}, and CO_3^{-} on the surfaces of smithsonite before and after co-activation with Pb^{2+} and STG prior to sulfidization. The results indicate that co-activation with Pb^{2+} and STG reduces the normalized peak intensity of CO_3^{-} on the smithsonite surface compared to direct sulfidization, with a more pronounced change. In contrast, the normalized peak intensities of Pb^{+} and S^{-} are significantly higher after Pb^{2+} and STG treatment than after Na_2S treatment alone. These findings suggest that the adsorption of sulfur species on the sulfidized surface is linked to the activity of sulfidization products on the smithsonite surface, which is higher after co-activation than before.

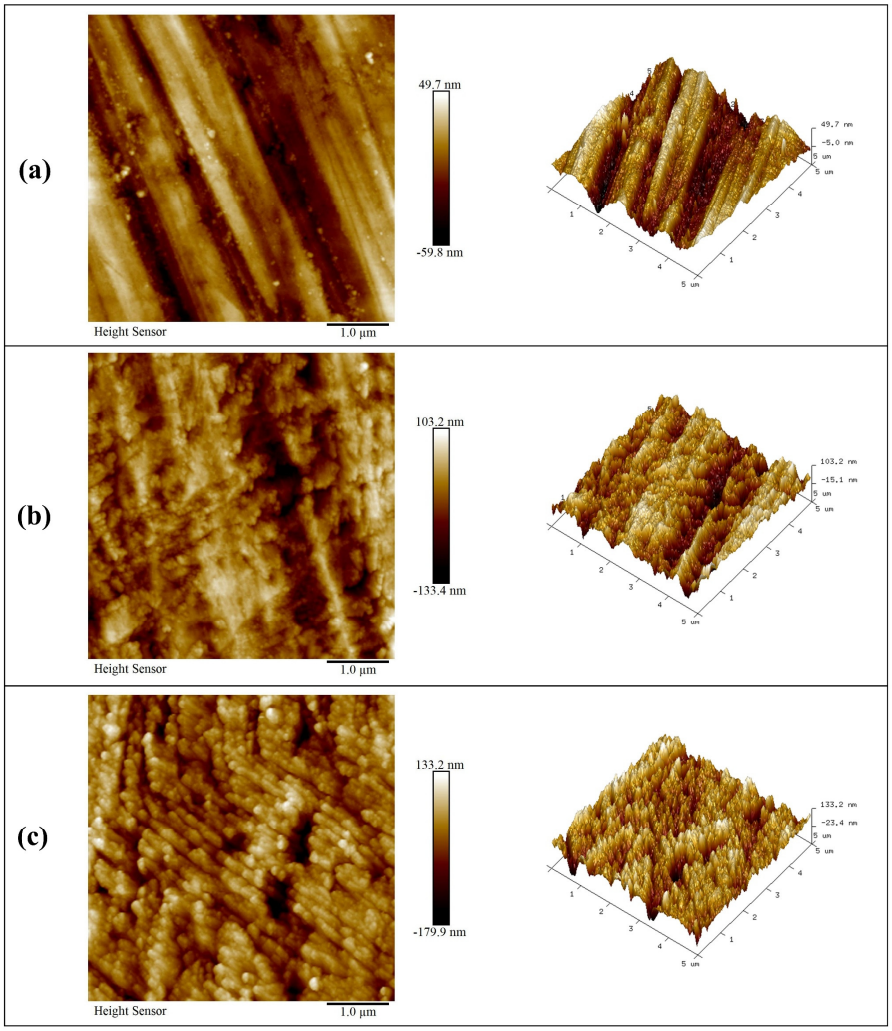

Figure 8. AFM surface morphology of smithsonite surface treated with (a) Water, (b) Na_2S, and (c) Pb^{2+}+ STG + Na_2S.

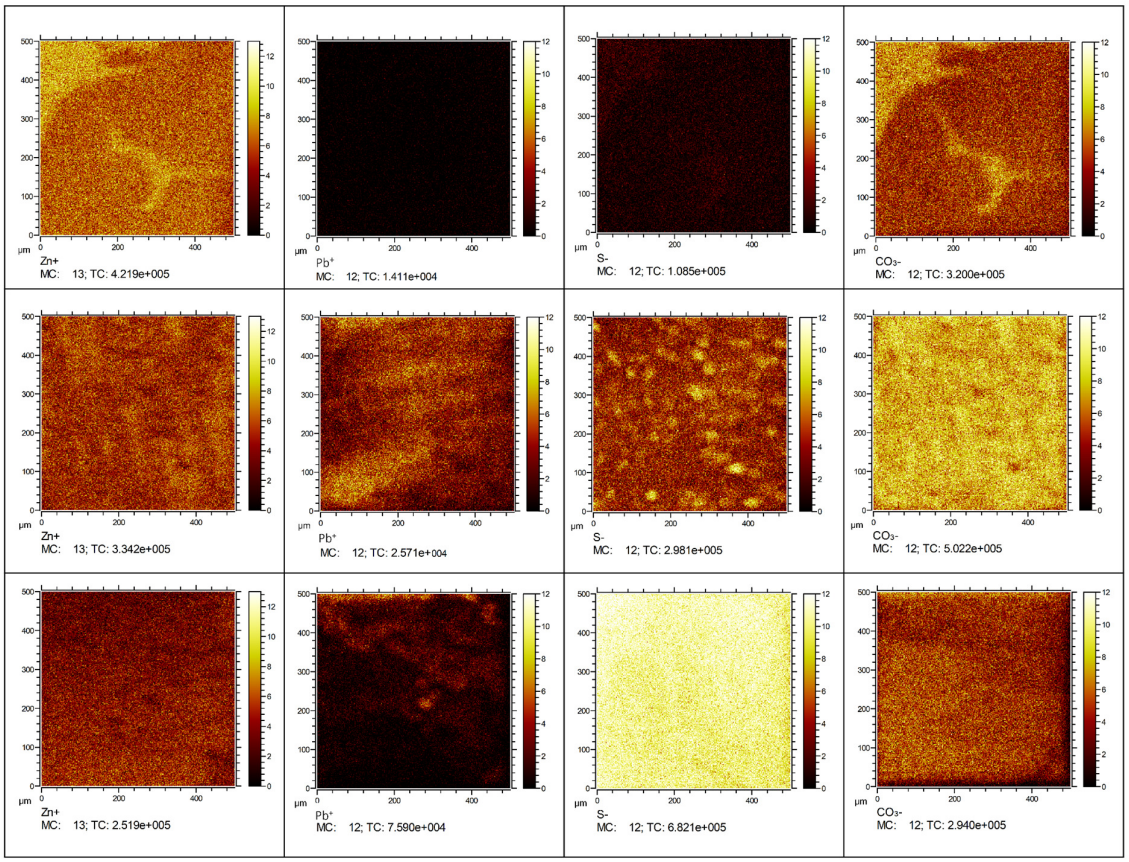

Figure 9. 2D distribution of ions on the smithsonite surface under the conditions of (a) Water, (b) Na_2S, and (c) Pb^{2+}+ STG + Na_2S.

3.6. EPMA test results

EPMA measurements were used to characterize the elemental distribution on the smithsonite surface after treatment under various conditions (as shown in Figure 11). The normalized mass of O, Zn, Pb, and S (as shown in Figure 12). For the water-treated smithsonite (as shown in Figure 11a), EPMA analysis revealed approximately 44.36 wt% O, 52.87 wt% Zn, and 0.26 wt% Pb, with no sulfur content detected on the surface, confirming the sample's relative purity (Figure 11a1, a2, a3, a4). After treatment with Na_2S (as shown in Figure 11b), the results showed a slight decrease in elemental content compared to the water-treated smithsonite, with 43.08 wt% O, 51.92 wt% Zn, and 0.23 wt% Pb (as shown in Figure 11b1, b2, b3). This decrease is likely due to the formation of sulfur compounds (e.g., ZnS) and elemental redistribution during Na_2S treatment. Sulfur (S) was detected on the surface at 0.86 wt% (as shown in Figure 11 b4), confirming the incorporation of sulfur and the formation of sulfur-containing compounds.

After smithsonite was co-activated with Pb^{2+} and STG prior to Na_2S treatment (as shown in Figure 11c), elemental content decreased to 41.39 wt% O and 49.35 wt% Zn (as shown in Figure 11c1, c2). Compared to the direct sulfidization of smithsonite, Pb increased by 6.67 wt% and sulfur by 1.59 wt%, indicating the formation of hydrophobic Pb-S and Zn-S films (as shown in Figure 11c3, c4). Accordingly, it was concluded that smithsonite was successfully activated and modified by Pb^{2+} and STG, thereby altering its surface chemistry and enhancing its reactivity and floatability. These findings suggest that the lead and sulfur compounds on the smithsonite surface form stable hydrophobic layers, improving the mineral's flotation properties and recovery.

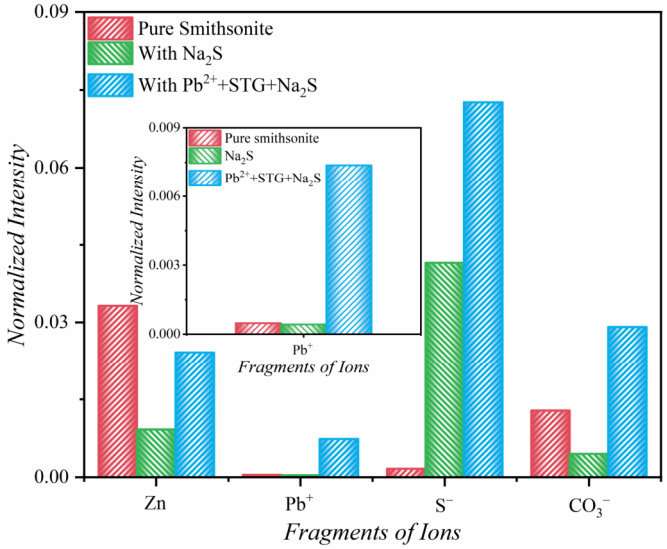

Figure 10. Normalized intensities of ion fragments on the smithsonite surface under the conditions of (a) Water, (b) Na_2S, and (c) Pb^{2+}+ STG + Na_2S.

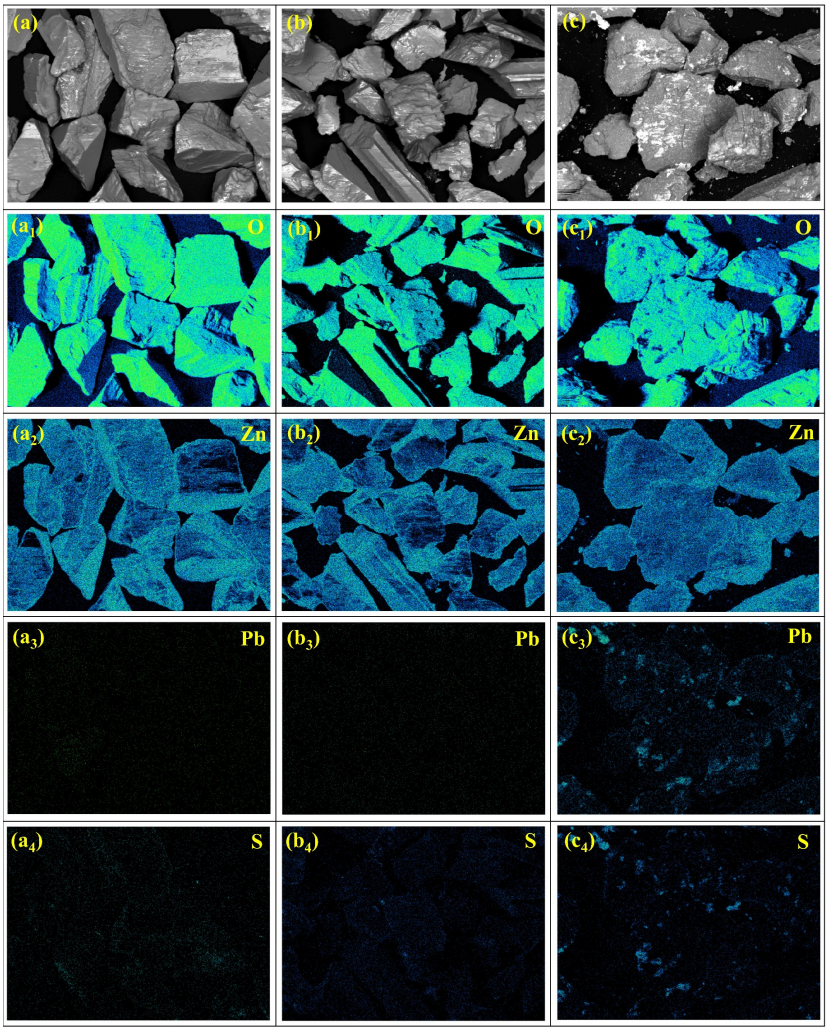

Figure 11. EPMA elemental maps of pure smithsonite treated with (a) Water, (b) Na_2S, and (c) Pb^{2+}+ STG + Na_2S.

3.7. ICP test results

Figure 13 shows the residual sulfur concentration in solution as a function of sulfidization time, both with and without the presence of Pb^{2+} and STG. When Na_2S was added to smithsonite, the sulfur concentration decreased from 27.38 mg/L to 8.60 mg/L after 10 minutes, indicating that only about 51.08% of the sulfur was initially attached to the smithsonite surface. This concentration increases over time, corresponding to a reduction in the residual sulfur concentration in the solution. This phenomenon, observed during sulfidization flotation of zinc and copper oxides, is attributed to the unstable adhesion of the formed products to the mineral surface [54,55]. After adding Pb^{2+} and STG before Na_2S, the sulfur concentration decreased from 9.57 mg/L to 3.42 mg/L after 6 minutes, with 71.49% of the sulfur mass adsorbed onto the smithsonite surface. Compared to direct sulfidization, co-activation increased sulfidization efficiency by 20%, as evidenced by lower sulfur residual concentrations in solution. These results are consistent with FESEM-EDS analysis, which shows increased sulfidized products on the smithsonite surface in the presence of Pb^{2+} and STG. After 8 minutes, the residual sulfur concentration began to rise, correlating with the detachment of sulfidized products from the surface.

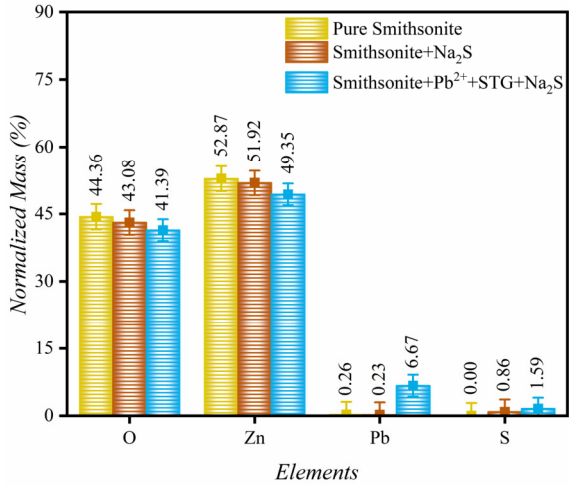

Figure 12. Normalized mass of pure smithsonite treated under various flotation conditions.

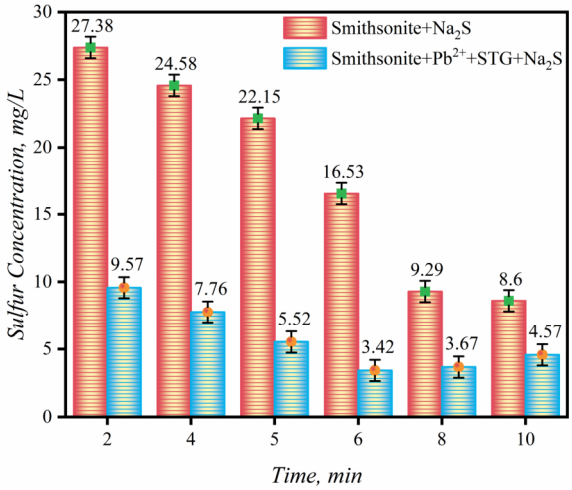

Figure 13. Sulfur concentration in solution as a function of sulfidization time in the presence or absence of Pb^{2+} and STG.

3.8. FT-IR test results

Fourier-transform infrared spectroscopy (FTIR) is an effective tool for analyzing the adsorption behavior of mineral surfaces [56]. To evaluate the impact of Pb^{2+} + STG co-activation and sulfidization on DDTC adsorption, FTIR analysis was performed on smithsonite samples under various conditions at pH 9. Figure 14 presents the FT-IR spectra of DDTC and smithsonite treated with different reagents. In the DDTC spectrum, peaks at 2975 cm^{-1} and 2924 cm^{-1} correspond to the symmetric C–H stretching vibrations of the methyl and methylene groups [57]. The peak at 1617 cm^{-1} is associated with the bending vibration of O–H in crystallized water [58]. The peak at 1406 cm^{-1} corresponds to the C–N vibration in the N–C=S group [59], and the range from 1257 to 1055 cm^{-1} is linked to C=S vibrations within the DDTC structure [60]. Peaks between 910 cm^{-1} and 830 cm^{-1} represent C–S vibrations [61]. In the FT-IR spectrum of smithsonite, the peak at 1400 cm^{-1} is attributed to the stretching vibration of −OH and the Vas (CO_3^{2-}) group. The peaks at 868 cm^{-1} and 738 cm^{-1} correspond to the out-of-plane and in-plane bending vibrations of the CO_3^{2-} group in smithsonite [62–64]. After treatment with Na_2S-DDTC, the FT-IR spectrum displays characteristic C=S stretching vibrations from DDTC, along with C–O stretching at 1125 cm^{-1}, O–H stretching at 2487 cm^{-1}, and symmetric C–H stretching at 2921 cm^{-1} and 2845 cm^{-1}. Compared to pure smithsonite, the FT-IR spectrum of Na_2S-DDTC-treated smithsonite shows C=S stretching vibrations from DDTC, confirming its adsorption on the surface. However, there is minimal improvement in the mineral's hydrophobicity [65].

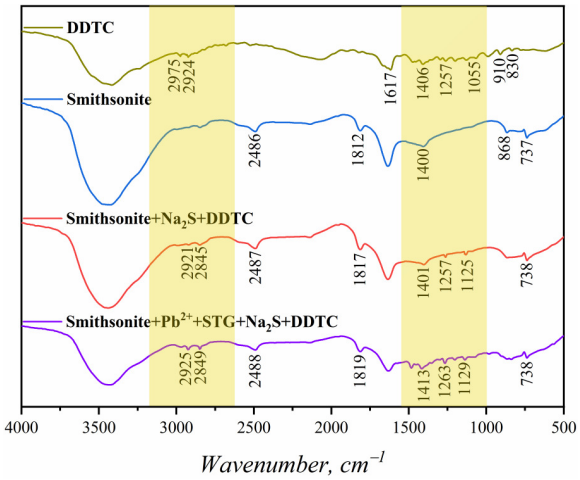

Figure 14. FT-IR spectra of smithsonite samples treated with different reagents.

After treatment with the Pb^{2+} + STG + Na_2S co-activation system, the intensity of the DDTC peaks in the FTIR spectra of smithsonite increased significantly. The highest intensity was observed with the Pb^{2+} + STG co-activation system, particularly when compared to Na_2S-DDTC-treated smithsonite. The peak at 1263 cm^{-1} corresponds to C=S stretching vibrations, indicative of the presence of DDTC. The intensity observed at this peak was higher than that seen in the Na_2S-DDTC treatment (1125 cm^{-1}). These results demonstrate that co-activation with Pb^{2+} + STG before adding Na_2S enhances DDTC adsorption on the smithsonite surface, resulting in greater surface hydrophobicity than direct sulfidization. Additionally, the C–H stretching vibration peaks of CH_2 and CH_3 at 2949 cm^{-1} and 2925 cm^{-1}, respectively, were enhanced, suggesting stronger chemisorption of xanthate species on the smithsonite surface in the Pb^{2+} + STG + Na_2S + DDTC system. This indicates a significant increase in smithsonite's surface activity, resulting in enhanced hydrophobicity across the entire surface. Based on the results and discussions mentioned above, the adsorption model for Pb^{2+} and STG on the smithsonite surface (as shown in Figure 15).

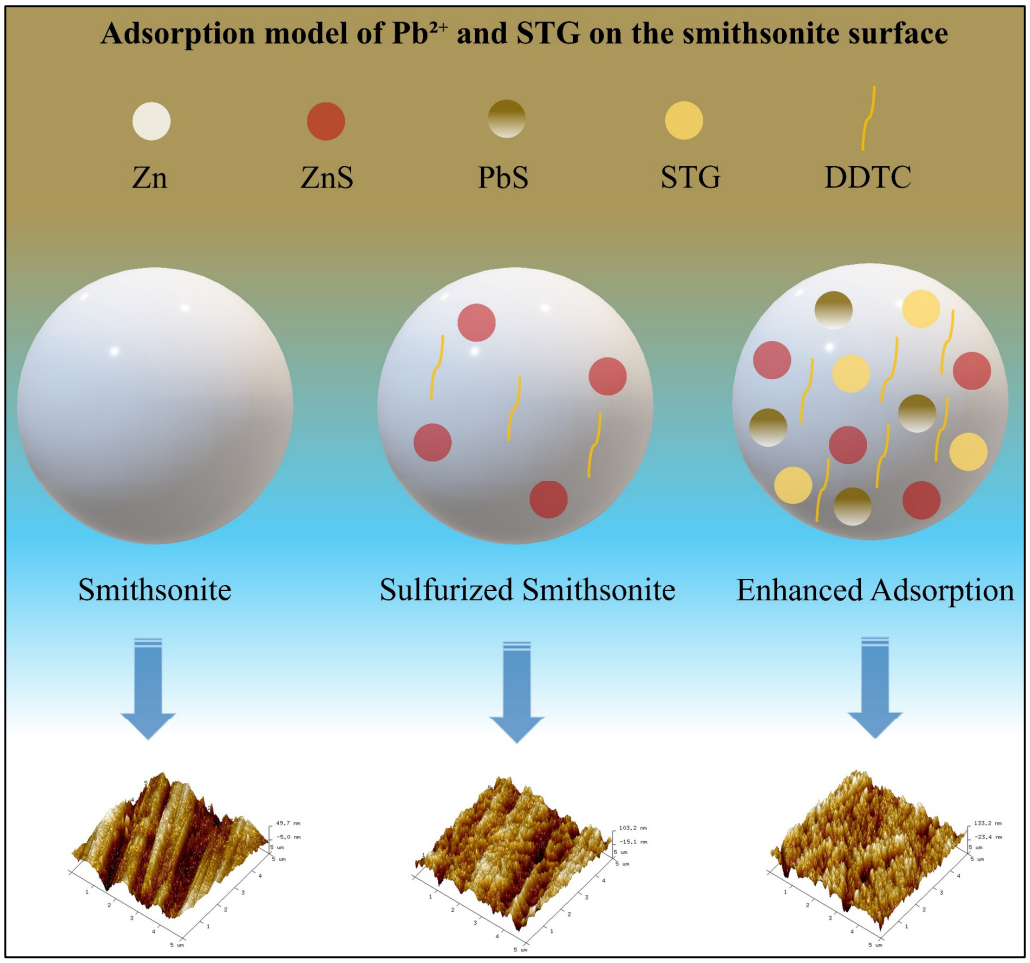

Figure 15. Adsorption model of Pb^{2+} and STG on the smithsonite surface.

4. Conclusions

This study investigated the effects of the co-activation mechanism of lead nitrate and sodium thioglycolate on the sulfidization-DDTC flotation system for smithsonite, focusing on the induced enhancement of sulfidization. The key findings are summarized as follows:

a) The XPS analysis showed that Pb^{2+} + STG co-activation enhances smithsonite sulfidization, promoting the formation of PbS and ZnS on the surface. FTIR analysis confirms that this co-activation enhances DDTC adsorption via C=S vibrations, increasing the number of active sites that interact with the collector.

b) The FESEM-EDS and AFM imaging at pH 9 confirmed that co-activating smithsonite with Pb^{2+} and STG before sulfidization enhances surface reactivity by forming dense Zn-S and Pb-S layers, increasing sulfur content, improving hydrophobicity, and strengthening DDTC interaction to promote flotation.

c) ToF-SIMS analysis indicated that the co-activation system significantly enhances reagent adsorption on smithsonite surfaces, showing increased Pb^{+} and S^{-} signal intensities compared to conventional sulfidization. The co-activation mechanism before sulfidization showed that Zn and Pb active sites were most abundant at concentrations of 2×10^{-3} mol/L Na_2S, 3×10^{-4} mol/L lead nitrate, and 3×10^{4} mol/L sodium thioglycolate, emphasizing their critical role. Without the co-activation mechanism, the recovery was significantly lower. The results confirmed an improvement in smithsonite recovery.

d) Flotation results analysis showed that the presence of lead nitrate and sodium thioglycolate, as a co-activation mechanism, significantly affected smithsonite floatability, achieving maximum recoveries of 89.32% and 93.19%, respectively, compared to direct sulfidization. Optimal reagent concentrations enhanced collector attachment, with DDTC having a stronger effect.

e) The combination of Pb^{2+} and STG in the co-activation system reduces reliance on Na_2S in industrial flotation, lowering both chemical and operational costs. This study suggests that STG may offer a more sustainable alternative, though further research is needed to evaluate its environmental impact fully.

Acknowledgments

This work was supported by the Central guidance local scientific and technological development funds (Grant No: 202407AB110022), National Natural Science Foundation of China (Grant No. 52074138), Caiyun Postdoctoral Program (Grant No. CG25066E003A).

References

[1]. Yang, T., Rao, S., Zhang, D., Wen, J., Liu, W., Chen, L., & Zhang, X. (2016). Leaching of low grade zinc oxide ores in nitrilotriacetic acid solutions. *Hydrometallurgy*, *161*, 107–111.

[2]. Ehsani, A., Ehsani, I., & Obut, A. (2021). Preparation of different zinc compounds from a smithsonite ore through ammonia leaching and subsequent heat treatment. *Physicochemical Problems of Mineral Processing, 57*, 96–106.

[3]. Cook, R. (2000). Connoisseur's Choice: Smithsonite, Tsumeb, Namibia. *Rocks & Minerals, 75,* 176–179.

[4]. Ding, W., Chen, Q., Li, Y., & Liu, X. (2023). Origins of Colour of Smithsonite from Yunnan, China. *Minerals 13,* 296.

[5]. Li, R., Shao, Y., Li, J., Liu, C., Chen, H., Meng, X., & Jia, X. (2024). Mechanism of Efficient Smithsonite Flotation with a Ternary Composite Collector Under Sulfur-Free Conditions. *Molecules, 29,* 6014.

[6]. Boryczko, B., Hołda, A., & Kolenda, Z. (2014). Depletion of the non-renewable natural resource reserves in copper, zinc, lead and aluminium production. *Journal of Cleaner Production, 84,* 313–321.

[7]. Daigo, I., Osako, S., Adachi, Y., & Matsuno, Y. (2014). Time-series analysis of global zinc demand associated with steel. *Resources, Conservation and Recycling, 82,* 35–40.

[8]. Chen, Y., Guo, X., & Chen, Y. (2023). Adsorption study of sesbania gum onto calcite surface: Implications for smithsonite-calcite flotation separation. *Colloids and Surfaces A: Physicochemical and Engineering Aspects, 676,* 132174.

[9]. Yan, L., Wang, A., Chen, Q., & Li, J. (2013). Dynamic material flow analysis of zinc resources in China. *Resources, Conservation and Recycling, 75,* 23–31.

[10]. Liu, C., Zhu, Y., Huang, K., Yang, S., & Liang, Z. (2021). Studies of benzyl hydroxamic acid/calcium lignosulphonate addition order in the flotation separation of smithsonite from calcite. *International Journal of Mining Science and Technology, 31,* 1153–1158.

[11]. Mehdilo, A., Irannajad, M., & Zarei, H. (2014). Smithsonite Flotation from Zinc Oxide Ore using Alkyl Amine Acetate Collectors. *Separation Science and Technology, 49,* 445–457.

[12]. Shi, Q., Feng, Q., Zhang, G., & Deng, H. (2012). Electrokinetic properties of smithsonite and its floatability with anionic collector. *Colloids and Surfaces*

A: Physicochemical and Engineering Aspects, 410, 178–183.

[13]. Xu, H., Wei, C., Li, C., Fan, G., Deng, Z., Zhou, X., & Qiu, S. (2012). Leaching of a complex sulfidic, silicate-containing zinc ore in sulfuric acid solution under oxygen pressure. *Separation Science and Technology, 85,* 206–212.

[14]. Xu, H., Wei, C., Li, C., Fan, G., Deng, Z., Li, M., & Li, X. (2010). Sulfuric acid leaching of zinc silicate ore under pressure. *Hydrometallurgy, 105,* 186–190.

[15]. Yang, K., Zhang, L., Lv, C., Peng, J., Li, S., Ma, A., Chen, W., & Xie, F. (2017). Role of sodium citrate in leaching of low-grade and multiphase zinc oxide ore in ammonia–ammonium sulfate solution. *Hydrometallurgy, 169,* 534–541.

[16]. Hosseini, S.H., & Forssberg, E. (2007). Physicochemical studies of smithsonite flotation using mixed anionic/cationic collector. *Minerals Engineering, 20,* 621–624.

[17]. Zhao, W., Yang, B., Yi, Y., Feng, Q., & Liu, D. (2023). Synergistic activation of smithsonite with copper-ammonium species for enhancing surface reactivity and xanthate adsorption. *International Journal of Mining Science and Technology, 33,* 519–527.

[18]. Moradi, S., & Monhemius, A.J. (2011). Mixed sulphide-oxide lead and zinc ores: Problems and solutions. *Minerals Engineering, 24,* 1062–1076.

[19]. Zhang, S., Wen, S., Liang, G., Xian, Y., & Chen, L. (2022). Ammonia pretreatment for enhancement of Pb ions adsorption on smithsonite surface and its flotation performance. *Applied Surface Science, 590,* 153069.

[20]. Liao, R., Wen, S., Liu, J., Bai, S., & Feng, Q. (2024). Experimental and molecular dynamics simulation study on DDA/DDTC mixed collector co-adsorption on sulfidized smithsonite surfaces. *Minerals Engineering, 205,* 108493.

[21]. Yang, J., Chen, L., Wu, D., & Zeng, J. (2023). Sodium sulfosalicylate activation mechanism on sulfidation flotation of smithsonite using dodecylamine as a collector. *Minerals Engineering, 192,* 107987.

[22]. Hosseini, S.H., & Forssberg, E. (2006). Adsorption studies of smithsonite flotation using dodecylamine and oleic acid. *Minerals & Metallurgical Processing, 23,* 87–96.

[23]. Pereira, C.A., & Peres, A.E.C. (2005). Reagents in calamine zinc ores flotation. *Minerals Engineering, 18,* 275–277.

[24]. Luo, B., Liu, Q., Deng, J., Yu, L., Lai, H., Song, C., & Li, S. (2019). Characterization of sulfide film on smithsonite surface during sulfidation processing and its response to flotation performance. *Powder Technology, 351,* 144–152.

[25]. Souza, T.F., & Lima, R.M.F. (2019). Cationic flotation of smithsonite and dolomite from Brazilian ambrósia norte deposit. *REM-International Engineering Journal, 72,* 619–624.

[26]. Önal, G., Bulut, G., Gül, A., Kangal, O., Perek, K.T., & Arslan, F. (2005). Flotation of Aladağ oxide lead-zinc ores. *Minerals Engineering, 18*, 279–282.

[27]. Wu, D., Wen, S., Deng, J., Liu, J., & Mao, Y. (2015). Study on the sulfidation behavior of smithsonite. *Applied Surface Science, 329,* 315–320.

[28]. Shi, Q., Zhang, G., Feng, Q., & Deng, H. (2013). Effect of solution chemistry on the flotation system of smithsonite and calcite. *International Journal of Mineral Processing, 119,* 34–39.

[29]. Ejtemaei, M., Gharabaghi, M., & Irannajad, M. (2014). A review of zinc oxide mineral beneficiation using flotation method. *Advances in Colloid and Interface Science, 206,* 68–78.

[30]. Wu, D., Ma, W., Wen, S., Deng, J., & Bai, S. (2017). Enhancing the sulfidation of smithsonite by superficial dissolution with a novel complexing agent. *Minerals Engineering, 114,* 1–7.

[31]. Zhang, S., Wen, S., Xian, Y., Liang, G., & Li, M. (2021). Pb ion Pre-Modification enhances the sulfidization and floatability of smithsonite. *Minerals Engineering, 170,* 107003.

[32]. Zhang, S., Wen, S., Xian, Y., Zhao, L., Feng, Q., Bai, S., Han, G., & Lang, J. (2019). Lead ion modification and its enhancement for xanthate adsorption on smithsonite surface. *Applied Surface Science, 498,* 143801.

[33]. Luo, Y., Ou, L., Zhang, G., Chen, J., Luo, Y., Zhou, H., Yang, H., & Yin, C. (2022). Unveiling the role of Ca ion in the sulfidation of smithsonite: A density functional theory study. *Journal of Molecular Liquids, 367,* 120485.

[34]. Jia, K., Feng, Q., Zhang, G., Ji, W., Zhang, W., & Yang, B. (2018). The role of S(II) and Pb(II) in xanthate flotation of smithsonite: Surface properties and mechanism. *Applied Surface Science, 442,* 92–100.

[35]. Bai, S., Li, C., Fu, X., Ding, Z., & Wen, S. (2018). Promoting sulfidation of smithsonite by zinc sulfide species increase with addition of ammonium chloride and its effect on flotation performance. *Minerals Engineering, 125,* 190–199.

[36]. Feng, Q., Wang, M., Zhang, G., Zhao, W., & Han, G. (2023). Enhanced adsorption of sulfide and xanthate on smithsonite surfaces by lead activation and implications for flotation intensification. *Separation & Purification Technology, 307,* 122772.

[37]. Xiao, Y., Peng, S., Tong, X., Xie, R., & Ma, Y. (2025). Enhancing the separation of galena from sphalerite by the synergistic effect of calcium oxide and sodium thioglycolate. *Colloids and Surfaces A:*

Physicochemical and Engineering Aspects, 720, 137189.

[38]. Smart, R.S.C., Skinner, W.M., & Gerson, A.R. (1999). XPS of Sulphide Mineral Surfaces : Metal-deficient, Polysulphides, Defects and Elemental Sulphur. *Surface and Interface Analysis, 105,* 101–105.

[39]. Herron, S.M., Lawal, Q.O., & Bent, S.F. (2015). Polysulfide ligand exchange on zinc sulfide nanocrystal surfaces for improved film formation. *Applied Surface Science, 359,* 106–113.

[40]. Lau, W.M., Kwok, R.W.M., & Ingrey, S. (1992). Controlling surface band-bending of InP with polysulfide treatments. *Surface Science, 271,* 579–586.

[41]. Song, H.S., Park, M.G., Ahn, W., Lim, S.N., Yi, K.B., Croiset, E., Chen, Z., & Nam, S.C. (2014). Enhanced adsorption of hydrogen sulfide and regeneration ability on the composites of zinc oxide with reduced graphite oxide. *Chemical Engineering Journal, 253,* 264–273.

[42]. Chai, R., Liu, Y., Liu, Q., & Xin, J. (2021). Interaction mechanism of calcite and four representative organic molecules: Experiments and DFT study. *Colloids and Surfaces A: Physicochemical and Engineering Aspects, 612,* 125822.

[43]. Jin, D., Sun, R., Wang, G., Deng, J., & Zhang, X. (2023). Flotation separation of fluorite and calcite using anhydrous glucose and aluminum sulfate as a combined depressant. *Applied Surface Science, 624,* 157089.

[44]. Zhang, S., Xian, Y., Wen, S., & Liang, G. (2022). Enhancement of xanthate adsorption on lead-modified and sulfurized smithsonite surface in the presence of ammonia. *Minerals Engineering, 189,* 107872.

[45]. Zhang, Y., Zhao, W., Han, G., & Feng, Q. (2025). A novel activation method for regulating surface characteristics and flotation performance of smithsonite: XPS, SEM-EDS, AFM, ToF-SIMS and FT-IR studies. *Separation Purification Technology, 352,* 128276.

[46]. Zhao, W., Liu, D., Wen, S., & Feng, Q. (2019). Surface modification of hemimorphite with lead ions and its effect on flotation and oleate adsorption. *Applied Surface Science, 483,* 849–858.

[47]. Jia, K., Feng, Q., Zhang, G., Shi, Q., & Chang, Z. (2017). Understanding the roles of Na_2S and Pb(II)in the flotation of hemimorphite. *Minerals Engineering, 111,* 167–173.

[48]. Li, R., Shao, Y., Li, J., Liu, C., Chen, H., Meng, X., & Jia, X. (2025). Utilization of fluorine ions to improve the sulfidization process and flotation recovery of smithsonite. *Separation & Purification Technology, 376,* 134029.

[49]. Zhu, G., Zhao, Y., Zheng, X., Wang, Y., Zheng, H., & Lu, D. (2020). Surface features and flotation behaviors of spodumene as influenced by acid and alkali treatments. *Applied Surface Science, 507,* 145058.

[50]. Zuo, Q., Wu, D., Cao, J., Wang, Z., Shuming, W., Huang, L., & Chen, H. (2023). Surface modification of hemimorphite via double-complexation by ammonium fluoride and copper ion to promote sulfidation. *Applied Surface Science, 612,* 155797.

[51]. Guan, Z., Liao, R., Zhang, Y., Feng, Q., & Wen, S. (2024). Experimental and simulation study on the flotation separation of smithsonite from dolomite using phosphoryl carboxyl copolymer as a novel depressant. *Separation & Purification Technology, 346,* 127488.

[52]. Yang, W., Tang, Y., Huang, B., Han, G., & Feng, Q. (2025). Experimental and molecular dynamics simulation insights into enhanced flotation of sulfidized smithsonite in a Cu–Pb dual activation system. *Green and Smart Mining Engineering, 2,* 8–17.

[53]. Zhao, W., Wang, M., Yang, B., Feng, Q., & Liu, D. (2022). Enhanced sulfidization flotation mechanism of smithsonite in the synergistic activation system of copper–ammonium species. *Minerals Engineering, 187,* 107796.

[54]. Bai, X., Liu, J., Wen, S., Wang, Y., & Lin, Y. (2020). Effect of ammonium salt on the stability of surface sulfide layer of smithsonite and its flotation performance. *Applied Surface Science, 514,* 145851.

[55]. Cai, J., Ma, Y., Su, C., Lai, H., Shen, P., Liu, D., & Pei, B. (2023). New insight into enhancing sulfurization of azurite with ethylenediamine and its response to xanthate adsorption. *Journal of Molecular Liquids, 389,* 122865.

[56]. Grich, A., Bouzid, T., Naboulsi, A., Regti, A., El Himri, M., & El Haddad, M. (2024). Synthesis and optimization of activated carbon from Doum (Chamaerops humilis) fiber via pyrolysis-assisted H_3PO_4 activation for removal of bisphenol A and α-Naphthol. *Diamond and Related Materials, 145,* 111061.

[57]. Mohammadi, I., Shahrabi, T., Mahdavian, M., & Izadi, M. (2020). Cerium/diethyldithiocarbamate complex as a novel corrosion inhibitive pigment for AA2024-T3. *Scientific Reports, 10,* 1–15.

[58]. Mohammadi, I., Shahrabi, T., Mahdavian, M., & Izadi, M. (2021). Chemical modification of LDH conversion coating with diethyldithiocarbamate as a novel anti-corrosive film for AA2024-T3. *Journal of Industrial and Engineering Chemistry, 95,* 134–147.

[59]. Touati, S., & Meniai, A.H. (2012). Solvent extraction of Cu (II) from sulphuric acid by means of sodium diethyldithiocarbamate and characterization of the formed complex. *Theoretical Foundations of Chemical Engineering, 46,* 719–726.

[60]. Cordeiro, A.P., Feuser, P.E., Figueiredo, P.G., Da Cunha, E.S., Martinez, G.R., Machado-de-Ávila, R.A., Rocha, M.E.M., de Araújo, P.H.H., & Sayer, C. (2021). In vitro synergic activity of diethyldithiocarbamate and 4-nitrochalcone loaded in beeswax nanoparticles against

melanoma (B16F10) cells. *Materials Science and Engineering: C, 120,* 111651.

[61]. Mazur, K.L., Feuser, P.E., Valério, A., Poester Cordeiro, A., De Oliveira, Assolini, C.I., J.P., Pavanelli, W.R., Sayer, C., & Araújo, P.H.H. (2019). Diethyldithiocarbamate loaded in beeswax-copaiba oil nanoparticles obtained by solventless double emulsion technique promote promastigote death in vitro. *Colloids and Surfaces B: Biointerfaces, 176,* 507–512.

[62]. Henry, D.G., Watson, J.S., & John, C.M. (2017). Assessing and calibrating the ATR-FTIR approach as a carbonate rock characterization tool. *Sedimentary Geology, 347,* 36–52.

[63]. Sun, H., Niu, F., & Zhang, J. (2021). Investigation on the flotation separation of smithsonite from calcite using calcium lignosulphonate as depressant. *Colloids and Surfaces A: Physicochemical and Engineering Aspects, 630,* 127571.

[64]. Liu, W., Peng, X., Liu, W., Wang, X., Zhao, Q., & Wang, B. (2020). Effect mechanism of the iso-propanol substituent on amine collectors in the flotation of quartz and magnesite. *Powder Technology, 360,* 1117–1125.

[65]. Ibrahim, A.M., Wang, Elnabi, H., G., Yousif, J.A., & Liu, D. (2025). Effect of sodium diethyldithiocarbamate (DDTC) and xanthate collaborative collection in malachite sulfurization flotation: Enhancement and mechanisms. *Physicochemical Problems of Mineral Processing, 61,* 203078.

نشریه مهندسی معدن و محیط زیست
نشانی نشریه: www.jme.shahroodut.ac.ir
انجمن مهندسی معدن ایران
دانشگاه صنعتی شاهرود

مکانیسم فعال‌سازی همزمان نیترات سرب و تیوگلیکولات سدیم در فلوتاسیون سولفیداسیون اسمیت سونیت

ایمان ابراهیم[۱،۲،۳*]، هان وانگ[۱]، دیان‌ون لیو[۱]، پیلون شن[۱]، حسن عثمان[۳]، مهند الحاج[۴]، محمد ابراهیم[۴]، و مصباح خلیل[۴]

۱. آزمایشگاه کلیدی ایالتی بهره‌برداری پاک از منابع فلزی غیرآهنی پیچیده، یونان آزمایشگاه کلیدی جداسازی سبز و غنی‌سازی منابع فلزی استراتژیک، دانشکده مهندسی منابع زمین، دانشگاه علوم و فناوری کونمینگ، کونمینگ ۶۵۰۰۹۳، یونان، جمهوری خلق چین
۲. گروه مهندسی معدن، دانشکده علوم مهندسی، دانشگاه نیالا، نیالا ۶۳۳۱۱، جمهوری خلق سودان
۳. گروه شیمی، دانشکده آموزش، دانشگاه نیالا، نیالا ۶۳۳۱۱، سودان
۴. گروه مهندسی معدن، دانشکده علوم مهندسی، دانشگاه اسلامی امدورمان، خارطوم ۱۴۴۱۱، جمهوری خلق سودان

اطلاعات مقاله

تاریخ ارسال: ۲۰۲۵/۱۰/۲۷
تاریخ داوری: ۲۰۲۵/۰۲/۰۵
تاریخ پذیرش: ۲۰۲۵/۰۶/۱۱

DOI: 10.22044/jme.2026.17042.3355

کلمات کلیدی

اسمیت‌زونیت
مکانیسم هم‌فعال‌سازی
نیترات سرب
سدیم تیوگلیکولات
جذب

چکیده

در این مطالعه، از Pb^{2+} و STG به عنوان معرف‌های مؤثر فعال‌سازی همزمان قبل از عملیات سولفید سدیم برای ارزیابی تأثیر آنها بر قابلیت شناوری اسمیت‌زونیت استفاده شد. نتایج آزمایش شناورسازی نشان داد که غلظت‌های سدیم سولفید نونهیدرات (SSN) و سدیم دی‌اتیل دی‌تیوکاربامات (DDTC) به طور قابل توجهی بر قابلیت شناوری تأثیر می‌گذارند و به ترتیب به حداکثر بازیابی ۸۹.۳۲٪ و ۹۳.۱۹٪ دست می‌یابند. آنالیز XPS تأیید کرد که عملیات Na_2S گونه‌های گوگرد را به سطح اسمیت‌زونیت وارد می‌کند، اتصال به کلکتور را افزایش می‌دهد و تشکیل PbS و ZnS را تسهیل می‌کند. آنالیز FTIR همچنین ثابت کرد که فعال‌سازی همزمان، جذب DDTC را از طریق ارتعاشات C=S افزایش می‌دهد و در نتیجه تعداد مکان‌های فعال موجود برای تعامل با کلکتور را نسبت به سولفیداسیون مستقیم افزایش می‌دهد. آنالیز FESEM-EDS و AFM در pH 9 تأیید کردند که فعال‌سازی همزمان منجر به تشکیل لایه‌های متراکم‌تر و ابرمانند PbS و ZnS روی سطح می‌شود. این لایه‌ها راندمان شناورسازی را بهبود بخشیدند، آبگریزی را افزایش دادند و برهمکنش DDTC را تقویت کردند و در نتیجه شناورسازی را ارتقا دادند. علاوه بر این، آنالیزهای ToF-SIMS و EPMA شدت‌های بالاتر Pb+ و S- را در سیستم فعال‌سازی همزمان نشان دادند که نشان‌دهنده افزایش واکنش‌پذیری سطح و اثبات افزایش فعالیت و تنوع محصولات سولفیداسیون است. این مطالعه با بهینه‌سازی شیمی سطح و اتصال کلکتور، رویکردی مؤثر برای افزایش بازیابی شناورسازی اسمیت‌زونیت ارائه می‌دهد.

نویسنده مسئول مکاتبات: aymanzrouge@gmail.com (م. ابراهیم)